



Research paper

## Design of a Synchronous Reluctance Motor with New Hybrid Lamination Rotor Structure

R. Rouhani, S. E. Abdollahi\*, S. A. Gholamian

Electrical and Computer Engineering Dept., Babol Noshirvani University of Technology, Babol, Iran.

### Article Info

#### Article History:

Received 14 July 2022  
Reviewed 27 August 2022  
Revised 24 September 2022  
Accepted 22 October 2022

#### Keywords:

Synchronous reluctance motor  
Hybrid laminations design  
Anisotropic rotor  
Axial laminations  
Segmental laminations  
Average torque  
Torque ripple

\*Corresponding Author's Email  
Address: [e.abdollahi@nit.ac.ir](mailto:e.abdollahi@nit.ac.ir)

### Abstract

**Background and Objectives:** The rotor of synchronous reluctance machines (SynRM) is conventionally designed and implemented in two types of axially-laminated anisotropic (ALA) and transversely-laminated anisotropic (TLA). Torque ripple and power factor have always been the design challenges of this machine; however, with proper design, their values can be as close as possible to the desired value. Each of these two structures has some advantages over the other, in terms of electromagnetic performance and ease of construction. For the first time, in this paper, a hybrid anisotropic rotor is presented with both radial and axial laminations, based on the theory of anisotropic rotor structure for the fundamental harmonic and isotropic rotor structure for other harmonics, so that the designed motor meets the advantages of both structures as much as possible.

**Methods:** To this end, the proposed design is implemented and investigated a Magnetic Equivalent Circuit (MEC) for the first slot harmonic on a machine with stator of 24-slots. To evaluate the proposed design, its electromagnetic performance is simulated using Finite Element Method.

**Results:** The theory-based conceptual design method is applied to a rotor with new structure and simulation results including average torque, power factor and torque ripple of the machine are presented.

**Conclusion:** Based on the obtained simulation results and comparing performance of the proposed design with other structures, it is shown that there will be a significant improvement in electromagnetic features including torque ripple, average torque and power factor and the proposed design has lower torque ripple than ALA rotor and higher average torque and power factor than TLA rotor.

This work is distributed under the CC BY license (<http://creativecommons.org/licenses/by/4.0/>)



### Introduction

According to SynRM rotor geometry, anisotropic structure is typically created in two forms of ALA and TLA. This anisotropic structure is generated by an appropriate distribution of flux carriers (made of magnetic material) and flux barriers (made of non-magnetic material or air). The lack of magnets and winding on the rotor, in addition to the simplicity of the structure, leads to a reduction in the cost of material and the manufacturing and assembly process. The lack of magnets also reduces the machine

sensitivity to temperature and fault current, resulting a simpler control method, higher torque-to-current ratio, and the ability to tolerate short-term overload capability [1]- [3]. Various investigations have been carried out regarding ALA rotors during 1990s. Meanwhile, rotor laminations with high thickness [4] and low thickness (like the thickness of normal laminations applied in TLA rotors) [5] are investigated. The lamination thickness which is 1.56 mm in [6] is rather high. Although the major component of the magnetic field is constant relative to the rotor, higher-order flux harmonics in ALA rotors result

in eddy current loss in laminations, which can impose additional losses to the machine [7], [8].

Increasing the number of laminations below each pole leads to a decrease in torque ripple, as well as reduction in losses caused by harmonic flux densities [5], also better distribution of insulations and thus increasing their effect as a flux barrier in the rotor [9]. To reduce these losses, radial slits can be created in 2-4 locations on each lamination along the d-axis to increase the length of eddy current path [10]. In general, rotors with strong anisotropy structure are made possible by ALA topology using a large number of laminations [11]. The simplest structure for SynRM machine is investigated in [12], [13]. This structure was so simple in terms of magnetic and mechanical aspects. However, magnetically, this structure has torque ripple and iron rotor losses and low torque density. In [14] and [15], instead of insulation, flexible magnets and ferrites are respectively employed between laminations. In ALA, due to the absence of tangential ribs between flux carriers in the flux weakening zone, the stator flux decreases significantly and the saliency ratio increases remarkably, which eventually leads to improved power factor [14]. The rotor anisotropy of SynRM leads to high harmonics of airgap flux density, which makes its electromagnetic analytical modeling complicated. In this regard various analytical methods are employed in order to predict the d- and q- axis inductances as well as average torque and torque ripple. Commonly MEC is used to quickly evaluate machine average torque with an acceptable accuracy [16], [17]. Also, in order to increase its accuracy and capability to calculate the torque ripple, mixed MEC is coupled with conformal mapping and other analytical tools [18], [19].

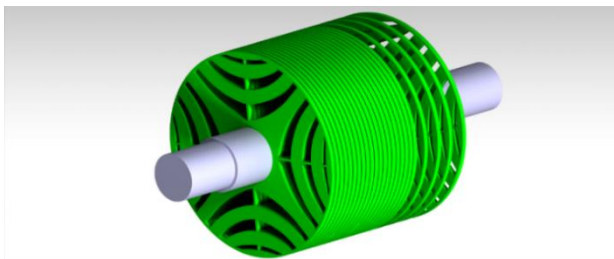


Fig. 1: Transversely-Laminated Anisotropic (TLA).

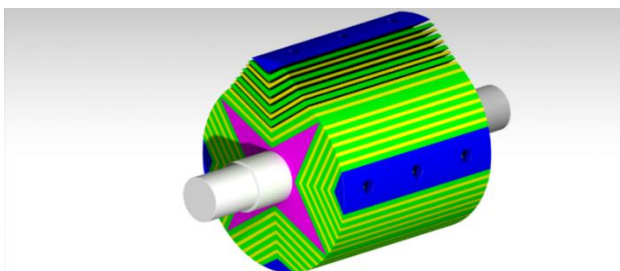


Fig. 2: Axially-Laminated Anisotropic (ALA).

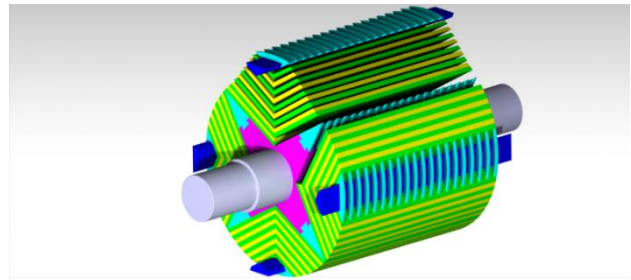


Fig. 3: Hybrid-laminated Anisotropic (HLA).

In this paper, based on the inductance theory regarding anisotropic rotors, a new structure is presented to achieve a high saliency ratio as well as the optimal torque ripple. This is the evolved version of conventional ALA and TLA structures. In this regard proposed structure is introduced first and then, analytically and numerically, shown that like ALA, it has a high saliency ratio (average torque and power factor) and, like TLA, has a desirable torque ripple. From this perspective, first, design parameters of ALA and TLA topologies are briefly reviewed. Then design fundamentals of the hybrid topology derived from the inductance theory in anisotropic rotors are presented, and finally, magnetic simulation of the proposed topology and its comparison with conventional ones are examined.

### Design Parameters of Anisotropic Rotor

The operating principles of SynRM are based on inductance change of each phase of the stator with rotation of rotor. The ratio of the maximum inductance to the minimum inductance is called saliency ratio, shown by  $\xi$ . This saliency ratio is optimized by coefficient of  $\alpha$  in ALA rotors, which is obtained by:

$$\alpha = \frac{W_i}{W_l} \tag{1}$$

in which  $W_i$  and  $W_l$  are insulation and lamination width, respectively.

The optimal value of  $\alpha$  coefficient of ALA topology is investigated in various literatures, such that, this coefficient is 0.59 in [5]; 0.5 in [10]; in order to reach the peak torque value, approximately 0.43 in [20]; to reach the peak of constant-power speed range (CPSR) approximately 0.67, and 1 in [8], [9], [21]. A comprehensive study of effect of changing  $\alpha$  coefficient from zero (isotropic rotor) to 1 on the inductance of d- & q-axes is carried out in [22], in which the optimal value of 0.5 is obtained. The smallness of  $\alpha$  coefficient means that more iron is employed in the core and accordingly, lower flux density, hence, reduction in losses due to the flux harmonics in the teeth.

Design method of TLA rotor geometry is brought in [3], [11], in which the saliency ratio depends on the number

and distribution of flux carriers and flux barriers in rotor [3], [23]. In general, the number of geometry design parameters of TLA rotor is greater than the number of ALA rotor parameters [24]; however, unequal size of lamination sheets cutting, assembly and ripple improvement techniques (such as skewing, etc.) in the ALA rotor is much more difficult [2]. The saliency ratio ( $\xi$ ) in TLA rotors is slightly lower than ALA rotor. Although in some literatures, saliency ratio in anisotropic rotors (especially ALA rotors) is estimated to be greater than 10 [10], [21], [25], [26], and even Kostko predicted it to be up to 25 in some structures. In loading condition, however, its saliency ratio is less than 10 [9].

**The Principles of Designing Hybrid-Laminated Rotor**

Anisotropic rotors (due to the presence of stator slots) have torque ripple inherently, because the fluxes existing inside and around the rotor change (in both amplitude and direction of bending of the flux) as they pass from one stator slot to another. Therefore, anisotropic rotors should be designed in a way that, in addition to approaching the highest saliency ratio, simultaneously has the highest uniformity of flux variations inside the rotor. SynRM machine inherently have high ripple, and for achieving optimal ripple, symmetric methods [3], [27] and asymmetric methods [24], [28], [29] are employed in TLA. In ALA, as mentioned earlier ripple can be slightly improved by considering the optimal  $\alpha$  coefficient and selecting the appropriate number of laminations.

In this paper, the  $\alpha$  coefficient for the axial laminations was considered to be 0.5, and as mentioned earlier, increasing the number of sheets in ALA, according to [5], leads to a decrease in torque ripple. Although ALA rotors have an almost smooth and circular surface, the holder section of the axial sheets around d and q axes is solid and made of non-magnetic material (Fig. 2); hence, ALA rotors have an inherent cutoff around q-axis. Although cutoff typically increases saliency ratio (hence average torque and power factor) [30], it significantly increases the torque ripple, too [31]. For this reason, TLA rotors are preferred over their longtime rival, i.e. ALA ones, because they have desired average torque, power factor, and torque ripple. Moreover, its manufacturing (cutting sheets with various dimensions and angles) and assembling process (mounting rotor sheets, assembly, and skewing the rotor) are easier than ALA.

Given in [32]-[34], d- and q-axes inductance and SynRM machine torque equation for the fundamental component are:

$$L_d(\theta) = L_{do} + \sum_{v=1}^{\infty} \Delta L_d \cos(vP N_s \theta) \tag{2}$$

$$L_q(\theta) = L_{qo} - \sum_{v=1}^{\infty} \Delta L_q \cos(vP N_s \theta) \tag{3}$$

$$L_{dq}(\theta) = - \sum_{v=1}^{\infty} \Delta L_{dq} \sin(vP N_s \theta) \tag{4}$$

$$T = \frac{m}{2} P [I_d I_q (L_{do} - L_{qo} + (\Delta L_d + \Delta L_q) \cos(P N_s \theta)) - (\Delta L_{dq} \sin(P N_s \theta) (I_d^2 - I_q^2))] - \frac{1}{2} P N_s [2 I_d I_q \Delta L_{dq} \cos(P N_s \theta) + I_d^2 \Delta L_d \sin(P N_s \theta) - I_q^2 \Delta L_q \sin(P N_s \theta)] \tag{5}$$

where  $v$ ,  $P$ ,  $N_s$ ,  $\vartheta$ , and  $m$  are Slot harmonic order, Machine’s pole pair number, Number of stator slots per pole pair, angle of rotor reference frame and Machine number of phases respectively. In (5) there are two terms of torque ripple components. The first terms,  $\Delta L_d$  and  $\Delta L_q$  are the inductance changes associated with each axis due to oscillations caused by the open stator slot (Carter's coefficient) as well as the rotating flux. The second term,  $\Delta L_{dq}$  is the mutual inductance changes between the stator and rotor teeth, which generates substantial torque oscillation.

In this paper, as shown in Figs. 4 & 5, these inductance variations could be reduced using proposed technique in a way that d & q axes of ALA rotor, separated by non-magnetic holders, and ultimately led to a lack of magnetic uniformity and solidity of the rotor, be modified by the radial laminated segments (TLA segmental).

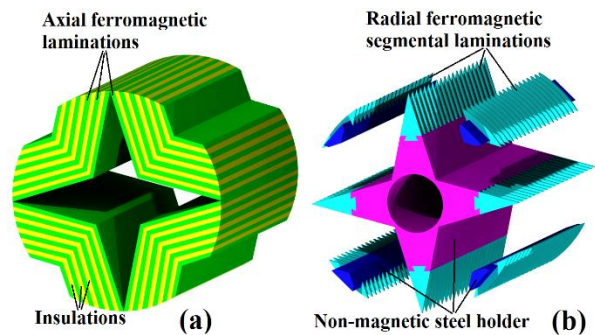


Fig. 4: The major sections of hybrid lamination rotor (a) ALA part (b) TLA part (segmental).

The design presented in Fig. 4-b, the d-axis segments are surrender and the q-axis segments surrounded on the holders.

The arrangement of d & q axes segments on the holders are not significantly different from each other magnetically, however, this is important due to the position of the segments and in order to have a better establishment and increase the mechanical strength and due to the limited space in the rotor.

Radial laminations which are segmentally established around d & q axes, ultimately have led the fluxes inside the rotor change less as they pass from one slot of the stator to another one, thus reducing the torque ripple.

Thus, the use of a rotor with two perpendicular laminations results in a structure with better peripheral uniformity while maintaining an anisotropic structure.

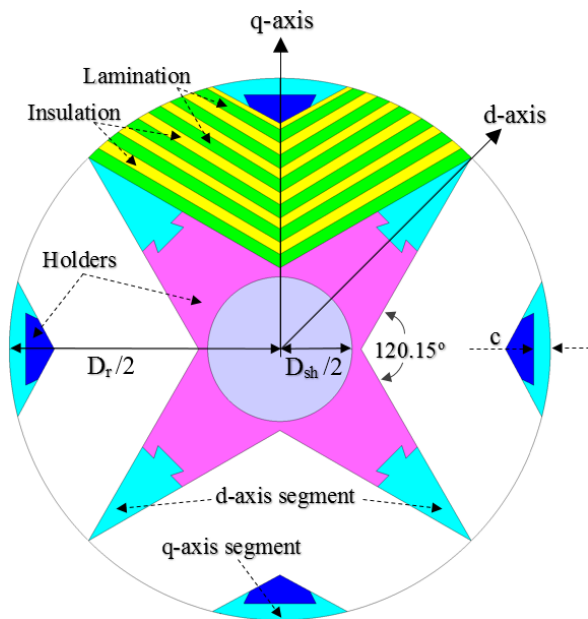


Fig. 5: Geometrical parameters of HLA rotor.

### Simulation of Magnetic Performance

Improving the magnetic performance of a machine and achieving a structure that simultaneously has all the desired parameters is always one of the main design objectives, which is, in some cases, impossible to achieve, or it's necessary to reconcile a number of parameters in multi-objective functions and its optimization.

To verify that the proposed topology provides all the intended electromagnetic parameters adequately, a 1500-watt induction motor stator was used, the rotor of which was replaced by three different rotors with ALA, TLA and HLA topologies, and the electromagnetic features of all three structures were examined and compared. The geometric parameters of the stator and all three rotors are listed in Table 1. A diagram of developed electromagnetic torque related to all three rotor topologies is displayed in Fig. 9.

HLA performance features, shown in Table 2, suggest that the proposed design can be effective in performance improvement of average torque, power factor, and torque ripple.

In other words, the best design for anisotropic rotors is to have the highest saliency ratio (anisotropic feature) along with the least amount of variations in terms of stator teeth for rotor rotation as large as a polar step of the rotor, so that it leads to maximum average torque and minimum torque ripple, respectively.

Flux density distribution of TLA, ALA and HLA rotors are shown in Figs. 6, 7, and 8 respectively.

Table 1: Design characteristics of the SynRM

Common Parameter	value
Rated power	1.5 (kw)
Air gap	0.5 (mm)
Stator outer diameter	140 (mm)
Stack length	90 (mm)
$S_{so}$	2.5 (mm)
$n_s$	24
Nominal current	4.5 (A)
Based speed	1500 (rpm)
Number of turns per slot	76
$D_{sh}$	24 (mm)
Magnetic Sheet	M400-50A
TLA Rotor	
$N_b$	3
$D_r$	90 (mm)
$R_{so}$	3.3 (mm)
$TR_x$	1 (mm)
$RR_x$	1 (mm)
$\alpha_1$	11.6 (deg)
$k_{wq}$	0.8
ALA Rotor	
$W_i$	0.25 (mm)
$W_l$	0.5 (mm)
HLA Rotor	
$C$	2.75 (mm)

Table 2: Comparison of the electromagnetic characteristic of SynRM with TLA, ALA AND HLA rotor

Unit	Parameter	TLA	ALA	HLA
Nm	$T_{av}$	11.01	13.07	12.6
%	$\Delta T$	7.63	23.48	9.12
A	$I$	4.5	4.5	4.5
Nm/A	$T/A$	2.44	2.90	2.8
mH	$L_d$	329.53	317.50	326.57
mH	$L_q$	98.64	59.66	67.99
---	$\xi$	3.34	5.32	4.80
---	PF	0.539	0.684	0.655

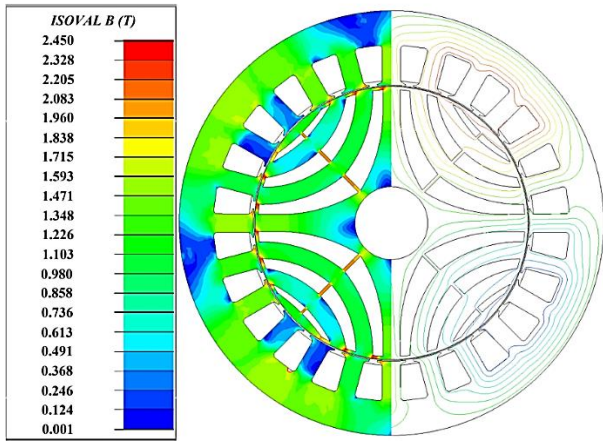


Fig. 6: Flux density distribution of TLA rotor in 4.5A current.

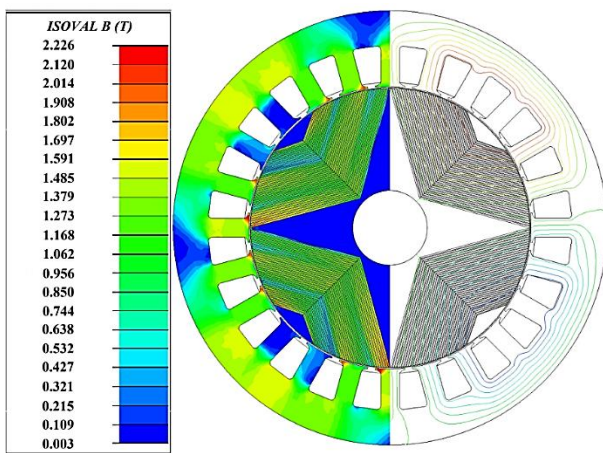


Fig. 7: Flux density distribution of ALA rotor in 4.5A current.

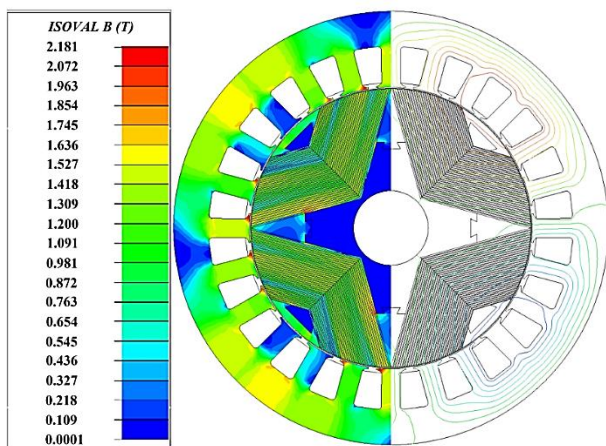


Fig. 8: Flux density distribution of HLA rotor in 4.5A current.

A. Magnetic Simulation Results

The effect of the d & q axes segments on the torque and inductance characteristics of each phase, are separately shown in Figs. 9, 10, and 11, respectively. It is observed that if the segments only affect the d-axis, since this segment is in the path of the q-axis fluxes, the loops

of the q-axis fluxes are closed in a more uniform path. According to (3), by the rotor rotation, the flux changes in the peripheral areas of the rotor decreases as it passes from one stator slot to another, resulting in a lower flux variation of q-axis and ultimately, the lower inductance variations of torque ripple generator of q-axis ( $\Delta L_q$ ).

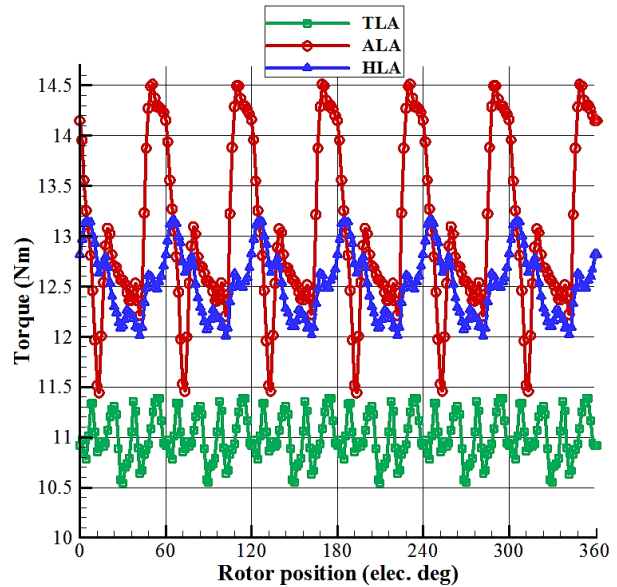


Fig. 9: Torque characteristics of SynRM with TLA, ALA & HLA rotors.

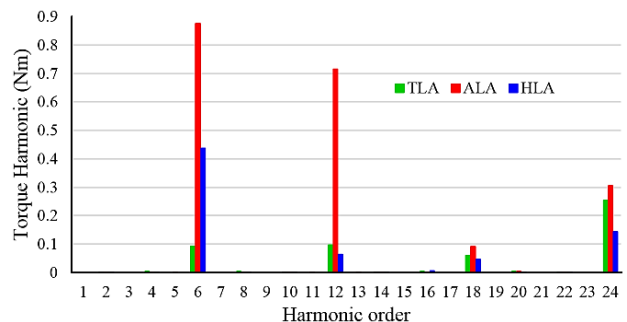


Fig. 10: Harmonic components of the torque ripple.

If the segments only affect the q-axis, because this segment is in the path of the d-axis fluxes, the loops of the d-axis flux are closed in a more uniform path. According to (2), by the rotor rotation, flux changes in the surrounding areas of the rotor decreases as it passes from one stator slot to another, resulting in a lower flux variation of d-axis and ultimately, the lower inductance variations of torque ripple generator of d-axis ( $\Delta L_d$ ). On the other hand, the presence of a non-magnetic holder around the q-axis in ALA topology leads to  $\Delta L_{dq}$ . This quantity is produced due to simultaneous distance or approach of the holder end to the stator teeth. By placing magnetic segments around the q-axis, the rotor has more uniform external areas, resulting in reduced mutual inductance that changes between the stator and rotor

teeth. Therefore, according to Table 2 and Fig. 9, torque ripple reduction in HLA topology is greater than torque ripple reduction in ALA.

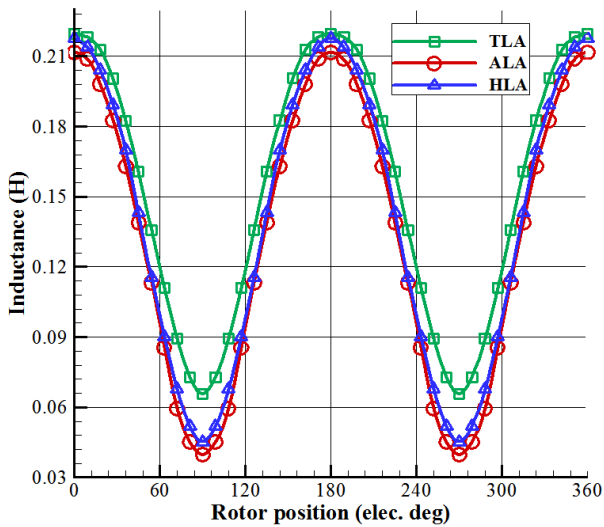


Fig. 11: Phase inductance variation of SynRM with TLA, ALA & HLA rotors.

In Fig. 11, the phase inductance variations for ALA, TLA, and HLA rotors for an electrical cycle are shown. It can be seen that the  $L_{\text{phase-max}}$  of the HLA rotor is almost equal to the  $L_{\text{phase-max}}$  of the TLA rotor and the  $L_{\text{phase-min}}$  of the HLA rotor is almost equal to the  $L_{\text{phase-min}}$  of the ALA rotor. From the Fig. 11 and Table 2, it can be found that HLA, in addition to having average torque and higher power factor, its ripple is almost the same as TLA. It also requires less magnetization current, hence its copper losses and machine torque density would improve.

The inductance of each phase is achieved by Finite Element Software, and for transferring this inductance to rotor reference frame, it should be multiplied by 1.5. Therefore, given in [4], [35], the d- & q-axes inductances, are obtained by:

$$L_d = \frac{3}{2} L_{\text{phase-max}} \tag{6}$$

$$L_q = \frac{3}{2} L_{\text{phase-min}} \tag{7}$$

where  $L_{\text{phase-max}}$  and  $L_{\text{phase-min}}$  are Inductances of each phase for the maximum rated current in the direction of the d and q rotor axis respectively. The saliency ratio is obtained:

$$\xi = \frac{L_d}{L_q} \tag{8}$$

Given [9], [22], the maximum power factor is equal to:

$$PF_{\text{max}} = \frac{\xi - 1}{\xi + 1} = \frac{L_d - L_q}{L_d + L_q} \tag{9}$$

Since in addition to the fundamental component of flux density, the spatial and slot harmonics also flow in the

rotor, this flux manifests itself as torque ripple, shown in Figs. 9 and 10.

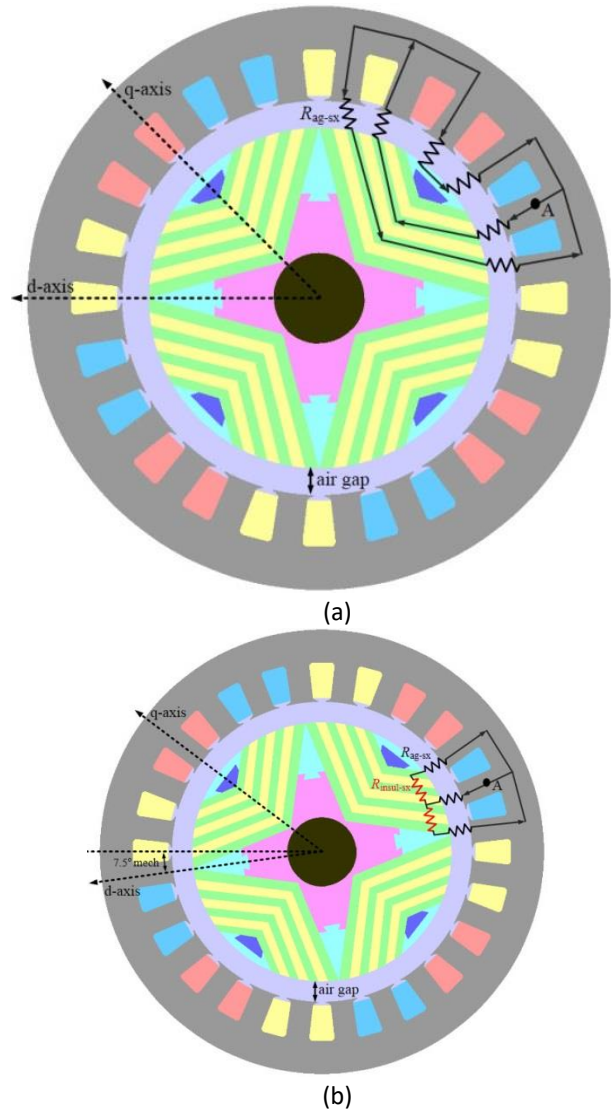


Fig. 12: The magnetic equivalent circuit of the passage of fluxes from each stator tooth to other teeth through the rotor path a) The magnetic reluctance of the d axis from the point of view of the A tooth- $R_{SA-d}$  b) The magnetic reluctance of the q axis from the point of view of the A tooth- $R_{SA-q}$ .

### B. The Performance Theory of the Proposed Rotor

In other publications, various magnetic equation circuits are modeled for synchronous reluctance motors, usually based on the fundamental component of the machine's torque-generating magnetic field, but these circuits do not have the desired capability to describe other harmonic components and their lateral issues. If the magnetic equivalent circuit is studied and modeled for the smallest region (a stator tooth and its flux flow path through the rotor and air gap), then the harmonic behavior of the machine can be predicted and evaluated in the final results.

Designers' approach to designing the geometry of electric machines from the point of view of harmonics (except for the fundamental harmonic) can be generally based on three axes; First, the machine parameters should be designed in such a way that almost no asynchronous harmonics (space and slot harmonics) are produced (for example, with a significant increase in the number of stator slot or a machine without teeth or stator core). Second, the machine parameters should be designed to decrease the amplitude of the asynchronous harmonics (for example, using the windings method of the chorded pitch or fractional slot). Third, the machine parameters should be designed so that the most effective slot harmonic of a pole pair is opposite the adjacent pole pair to be deleted (for example, rotor with asymmetric flux barrier geometry).

However, the design of the rotor of electric machines can be such that the rotor structure is anisotropic for the fundamental component of the rotating magnetic field and isotropic for other harmonic components so that the harmonic components of the rotor and stator have no interaction with each other. In SynRM, the most effective harmonic in the torque ripple characteristic is the first order of slot harmonics. Since all torque-ripple harmonic components, both space and slot harmonics, eventually have to flow through the stator teeth and close their way through the air gap and the rotor, it seems better to be modeled the possible flux paths from the point of view of just one stator tooth.

As shown in Fig. 12, since the cycle of the slot harmonic is 15 mechanical degrees and the  $R_{SA-d}$  and  $R_{SA-q}$  are 180 electrical degrees different from each other, in Fig. 12(a), (b) the rotor is rotated for 7.5 mechanical degrees. With proper design of the rotor structure, an isotropic path can be created from the A-tooth view for different rotor positions. Considering the changes in magnetic reluctance ( $dR / d\theta$ ) and considering the passage of fluxes from each stator tooth to other teeth through the rotor path, the magnetic equivalent circuit for each stator tooth is shown in Fig. 12. Therefore, to minimize the torque ripple ( $dR / d\theta$ ), it is sufficient that the magnetic reluctance seen from the d and q axes for the first slot harmonic component of the stator from the point of view of each stator tooth (eg tooth A) is studied and the rotor should be designed to be  $R_{SA-d} \approx R_{SA-q}$ . Therefore, regardless of the magnetic resistance of the iron part of the stator and rotor:

$$R_{SA-d} = 3 R_{ag-sx} \tag{10}$$

$$R_{SA-q} = 1.5 R_{ag-sx} + 0.5 R_{insul-sx} \tag{11}$$

$$R_{SA-d} \approx R_{SA-q} \Rightarrow 3 R_{ag-sx} \approx R_{insul-sx} \tag{12}$$

where  $R_{SA-d}$ ,  $R_{SA-q}$ ,  $R_{ag-sx}$ , and  $R_{insul-sx}$  are magnetic reluctance seen from the d and q axes, air gap magnetic reluctance and insulation magnetic reluctance from the point of view of each stator tooth respectively. This ensures that the changes in magnetic reluctance from the point of view of each stator tooth for rotation of the rotor in different positions are always minimal, and these values will be good starting points for the final design of the rotor geometry.

Therefore, for the HLA rotor, in the first place by selecting the appropriate number of laminations and insulations, also in the second place by replacing the ferromagnetic segments at the ends of the d and q axes of the rotor, an isotropic structure can be created and  $dR/d\theta$  and finally the torque ripple is reduced. In other words, in the proposed structure due to the lack of radial and tangential ribs, the average torque is higher than TLA, also due to the appropriate number of insulations and laminations and ferromagnetic segments around the d and q axes of the rotor (creating an isotropic environment for slot harmonics) torque ripple are significantly better than ALA and almost equal to TLA.

### C. Space Harmonic Effect

According to torque characteristics and Fig. 10, it is observed that HLA and TLA have the most desired performance. By referring to Fig. 10 and comparing the torque characteristics of the two TLA and HLA rotors, the 6<sup>th</sup> harmonic component available in the torque characteristics for the HLA rotor is significant. The 6<sup>th</sup> harmonics in the torque feature is caused by the 5<sup>th</sup> and 7<sup>th</sup> space harmonics [36]. These space harmonics can be improved by chorded winding. If the winding step is shortened by  $1/n$ , the winding coefficient ( $k_w$ ) of (13) should be affected by the number of the winding turns:

$$k_w = \sin\left(\frac{180}{2} * \left(1 - \frac{1}{n}\right)\right) \tag{13}$$

In this relation, n is the target space harmonic order for attenuation or elimination. In this paper, n=6 was considered for attenuation of space 5<sup>th</sup> and 7<sup>th</sup> harmonics (given the number of slots and stator poles).

The torque ripple characteristics (with chorded winding) for TLA and HLA rotors are shown in Figs. 13, 14. It is obvious that ripple of HLA had a significant improvement. Fig. 14 proves that this ripple improvement is due to a significant decrease in the 6<sup>th</sup> harmonic in torque ripple. As it was expected, chorded winding had no effect on slot harmonics. Therefore, since in torque ripple characteristics of SynRM with TLA rotor there is not any remarkable space harmonic, chorded winding plays an insignificant role in performance improvement of TLA rotor. Magnetic quantities of HLA and TLA rotors with chorded and full pitch windings are listed in Table 3.

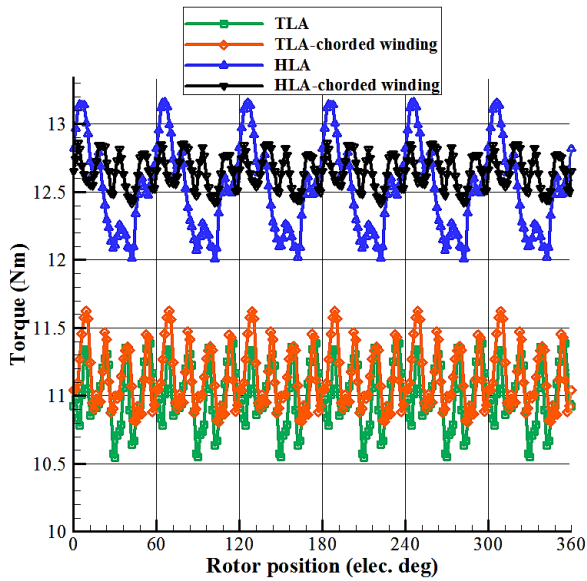


Fig. 13: A comparison of torque characteristics of HLA and TLA rotors with chorded and full pitch windings.

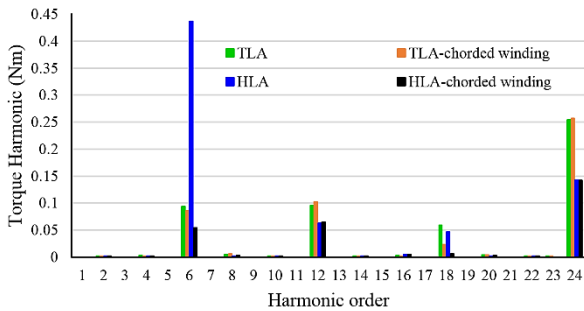


Fig. 14: Torque ripple harmonics components of SynRM with HLA and TLA rotors with chorded and full pitch windings.

Table 3: Comparison of the electromagnetic characteristic of SynRM with TLA, and proposed HLA rotor

		Different Rotor			
Unit	Parameter	TLA	TLA-chorded winding	HLA	HLA-chorded winding
Nm	$T_{av}$	11.01	11.13	12.6	12.65
%	$\Delta T$	7.63	7.34	9.12	3.5
A	$I$	4.5	4.5	4.5	4.5

**Conclusion**

Although ALA SynRM is not as widely recognized in the industry as TLA ones, it is further studied as hybrid lamination anisotropy in this paper and the possibility of improving its electromagnetic performance was confirmed. TLA has less ripple and simpler assembly and structure; nonetheless, ALA has some advantages such as higher power factor and average torque density than TLA. It is shown that proposed HLA exhibits moderate features

of both TLA and ALA rotors that although its torque ripple is a bit more than TLA but its average torque density and PF is modified. Also due to the magnetic characteristics of the desired torque, there is no need to any skewing to reduce torque ripple. Although HLA has more complex assembly than TLA, it has fewer design parameters, hence, it is easier for its optimization to achieve the desired electromagnetic characteristics.

**Author Contributions**

R. Rouhani collected the data, carried out the analysis and wrote paper, S. E. Abdollahi and S. A. Gholamian interpreted the results and supervised the research.

**Conflict of Interest**

The authors declare no potential conflict of interest regarding the publication of this work. In addition, the ethical issues including plagiarism, informed consent, misconduct, data fabrication and, or falsification, double publication and, or submission, and redundancy have been completely witnessed by the authors.

**Abbreviations**

- $W_i$  Insulation Width
- $W_l$  Lamination Width
- $L_d$  d- axis inductance
- $L_q$  q- axis inductance
- $L_{dq}$  Mutual inductance
- $L_{do}$  Constant amount of d-axis inductance
- $L_{qo}$  Constant amount of q-axis inductance
- $\nu$  Slot harmonic order
- $\Delta L_d$  Amplitude of changes of d-axis inductance
- $\Delta L_q$  Amplitude of changes of q-axis inductance
- $\Delta L_{dq}$  Fundamental amplitude mutual inductance
- $P$  Machine’s pole pair number
- $N_s$  Number of stator slots per pole pair
- $\vartheta$  Angle of rotor reference frame
- $m$  Machine number of phases
- $I_d$  d-axis current
- $I_q$  q-axis current
- $N_s$  Number of stator slots per pole pair
- $\xi$  Saliency ratio
- $R_{SA-d}$  d- axis magnetic reluctance from the point of view of each stator tooth
- $R_{SA-q}$  q- axis magnetic reluctance from the point of view of each stator tooth

$R_{ag-sx}$	Air gap magnetic reluctance from the point of view of each stator tooth
$R_{insul-sx}$	Insulations magnetic reluctance from the point of view of each stator tooth
$n$	Target space harmonic order
$k_w$	Winding coefficient
ALA	Axially-laminated anisotropic
TLA	Transversely-laminated anisotropic
CPSR	Constant-power speed range

## References

- [1] N. Bianchi, S. Bolognani, E. Carraro, M. Castiello, E. Fornasiero, "Electric vehicle traction based on synchronous reluctance motors," *IEEE Trans. Ind. Appl.*, 52: 4762-4769, 2016.
- [2] S. Taghavi, "Design of synchronous reluctance machines for automotive applications," Concordia University, 2015.
- [3] R. R. Moghaddam, F. Gyllensten, "Novel high-performance SynRM design method: An easy approach for a complicated rotor topology," *IEEE Trans. Ind. Electron.*, 61: 5058-5065, 2014.
- [4] Y. H. Kim, J. H. Lee, "Optimum design of ALA-SynRM for direct drive electric valve actuator," *IEEE Trans. Magn.*, 53(4): 1-4, 2017.
- [5] B. J. Chalmers, L. Musaba, "Design and field-weakening performance of a synchronous reluctance motor with axially laminated rotor," *IEEE Trans. Ind. Appl.*, 34: 1035-1041, 1998.
- [6] E. Obe, "Calculation of inductances and torque of an axially laminated synchronous reluctance motor," *IET Electr. Power Appl.*, 4: 783-792, 2010.
- [7] I. Scian, D. G. Dorrell, P. J. Holik, "Assessment of losses in a brushless doubly-fed reluctance machine," *IEEE Trans. Magn.*, 42: 3425-3427, 2006.
- [8] D. G. Dorrell, I. Scian, E. M. Schulz, R. B. Betz, M. Jovanovic, "Electromagnetic considerations in the design of doubly-fed reluctance generators for use in wind turbines," in *Proc. IECON 2006 - 32nd Annual Conference on IEEE Industrial Electronics: 4272-4277*, 2006.
- [9] D. Staton, T. Miller, S. Wood, "Maximising the saliency ratio of the synchronous reluctance motor," in *IEE Proceedings B (Electric Power Applications): 249-259*, 1993.
- [10] I. Boldea, Z. Fu, S. Nasar, "Performance evaluation of axially-laminated anisotropic (ALA) rotor reluctance synchronous motors," *IEEE Trans. Ind. Appl.*, 30: 977-985, 1994.
- [11] Y. Wang, G. Bacco, N. Bianchi, "Geometry analysis and optimization of PM-assisted reluctance motors," *IEEE Trans. Ind. Appl.*, 53: 4338-4347, 2017.
- [12] P. Lawrenson, L. Agu, "Theory and performance of polyphase reluctance machines," in *Proc. Institution of Electrical Engineers: 1435-1445*, 1964.
- [13] P. J. Lawrenson, S. Gupta, "Developments in the performance and theory of segmental-rotor reluctance motors," in *Proc. Institution of Electrical Engineers: 645-653*, 1967.
- [14] W. L. Soong, N. Ertugrul, "Field-weakening performance of interior permanent-magnet motors," *IEEE Trans. Ind. Appl.*, 38: 1251-1258, 2002.
- [15] I. Boldea, S. Nasar, "Emerging electric machines with axially laminated anisotropic rotors: a review," *Electr. Mach. power syst.*, 19: 673-703, 1991.
- [16] C. López, T. Michalski, A. Espinosa, L. Romeral, "Rotor of synchronous reluctance motor optimization by means reluctance network and genetic algorithm," in *Proc. 2016 XXII International Conference on Electrical Machines (ICEM): 2052-2058*, 2016.
- [17] C. López-Torres, A. G. Espinosa, J. R. Riba, L. Romeral, "c," *IEEE Trans. Veh. Technol.*, 67: 196-205, 2017.
- [18] M. Farhadian, M. Moallem, B. Fahimi, "Analytical calculation of magnetic field components in synchronous reluctance machine accounting for rotor flux barriers using combined conformal mapping and magnetic equivalent circuit methods," *J. Magn. Mag. Mater.*, 505: 166762, 2020.
- [19] A. Hanic, D. Zarko, D. Kuhinek, Z. Hanic, "On-load analysis of saturated surface permanent magnet machines using conformal mapping and magnetic equivalent circuits," *IEEE Trans. Energy Convers.*, 33: 915-924, 2018.
- [20] W. L. Soong, D. A. Staton, T. J. Miller, "Design of a new axially-laminated interior permanent magnet motor," *IEEE Trans. Ind. Appl.*, 31: 358-367, 1995.
- [21] D. Platt, "Reluctance motor with strong rotor anisotropy," *IEEE Trans. Ind. Appl.*, 28: 652-658, 1992.
- [22] T. Matsuo, T. A. Lipo, "Rotor design optimization of synchronous reluctance machine," *IEEE Trans. Energy Convers.*, 9: 359-365, 1994.
- [23] M. Ferrari, N. Bianchi, E. Fornasiero, "Analysis of rotor saturation in synchronous reluctance and PM-assisted reluctance motors," *IEEE Trans. Ind. Appl.*, 51: 169-177, 2015.
- [24] E. Howard, M. J. Kamper, S. Gerber, "Asymmetric flux barrier and skew design optimization of reluctance synchronous machines," *IEEE Trans. Ind. Appl.*, 51: 3751-3760, 2015.
- [25] E. C. F. Lovelace, "Optimization of a magnetically saturable interior permanent-magnet synchronous machine drive," Massachusetts Institute of Technology, 2000.
- [26] N. Bianchi, B. J. Chalmers, "Axially laminated reluctance motor: analytical and finite-element methods for magnetic analysis," *IEEE Trans. Magn.*, 38: 239-245, 2002.
- [27] S. Taghavi, P. Pillay, "A novel grain-oriented lamination rotor core assembly for a synchronous reluctance traction motor with a reduced torque ripple algorithm," *IEEE Trans. Ind. Appl.*, 52: 3729-3738, 2016.
- [28] M. Sanada, K. Hiramoto, S. Morimoto, Y. Takeda, "Torque ripple improvement for synchronous reluctance motor using an asymmetric flux barrier arrangement," *IEEE Trans. Ind. Appl.*, 40: 1076-1082, 2004.
- [29] M. Ferrari, N. Bianchi, A. Doria, E. Fornasiero, "Design of synchronous reluctance motor for hybrid electric vehicles," *IEEE Trans. Ind. Appl.*, 51: 3030-3040, 2015.
- [30] M. J. Kamper, A. Volsdhenk, "Effect of rotor dimensions and cross magnetisation on Ld and Lq inductances of reluctance synchronous machine with cageless flux barrier rotor," *IEE J. Electr. Power Appl.*, 141: 213-220, 1994.
- [31] R. Rajabi Moghaddam, "Synchronous reluctance machine (SynRM) in variable speed drives (VSD) applications," KTH Royal Institute of Technology, 2011.
- [32] A. Vagati, G. Franceschini, I. Marongiu, G. Troglia, "Design criteria of high performance synchronous reluctance motors," in *Proc. Conference Record of the 1992 IEEE Industry Applications Society Annual Meeting: 66-73*, 1992.
- [33] A. Fratta, G. Troglia, A. Vagati, F. Villata, "Evaluation of torque ripple in high performance synchronous reluctance machines," in *Proc. Conference Record of the 1993 IEEE Industry Applications Society Conference Twenty-Eighth IAS Annual Meeting: 163-170*, 1993.
- [34] S. A. Nasar, I. Boldea, *The induction machines design handbook: CRC press*, 2009.
- [35] K. C. Kim, J. S. Ahn, S. H. Won, J. P. Hong, J. Lee, "A study on the optimal design of SynRM for the high torque and power factor," *IEEE Trans. Magn.*, 43: 2543-2545, 2007.
- [36] A. Vagati, M. Pastorelli, G. Franceschini, S. C. Petrace, "Design of low-torque-ripple synchronous reluctance motors," *IEEE Trans. Ind. Appl.*, 34: 758-765, 1998.

## Biographies



**Rouhollah Rouhani** was born in Mahmudabad, Iran, in 1989. He received the M.Sc. degree from Babol Noshirvani University of Technology, Babol, Iran, in 2017. He is interested in electric machines topics.

- Email: [rouhollah.rouhani68@gmail.com](mailto:rouhollah.rouhani68@gmail.com)
- ORCID: NA
- Web of Science Researcher ID: NA
- Scopus Author ID: NA
- Homepage: NA



**Seyed Ehsan Abdollahi** was born in Sari, Iran. He received the B.Sc. degree from the Amirkabir University of Technology, Tehran, Iran, in 2002, the M.Sc. degree from Iran University of Science and Technology, Tehran, Iran, in 2005, and the Ph.D. degree from University of Tehran, Tehran, Iran, in 2014, all in Electric Power Engineering. He joined the Babol Noshirvani University of Technology, Babol, Iran, as an Assistant Professor. His current research interests include electric machine design and modeling, electric vehicle and power electronics.

- Email: [s.ehsan.abdollahi@gmail.com](mailto:s.ehsan.abdollahi@gmail.com)
- ORCID: [0000-0003-2277-1060](https://orcid.org/0000-0003-2277-1060)
- Web of Science Researcher ID:
- Scopus Author ID:
- Homepage: <https://ostad.nit.ac.ir/home.php?sp=390065>



**Sayyed Asghar Gholamian** was born in Babolsar, Iran, in 1976. He received his B.Sc. degree in electrical engineering from K.N. Toosi University of Technology, Tehran, Iran in 1999 and his M.Sc. degree in electric power engineering from the University of Mazandaran, Babol, Iran in 2001. He also received his Ph.D. in electrical engineering from K.N. Toosi University of Technology, Tehran, Iran in 2008. He is currently Assistant Professor in the Department of Electrical Engineering at the Babol University of Technology, Iran. His research interests include power electronic and design, simulation, modeling, and control of electrical machines.

- Email: [gholamian@nit.ac.ir](mailto:gholamian@nit.ac.ir)
- ORCID: [0000-0001-7654-7668](https://orcid.org/0000-0001-7654-7668)
- Web of Science Researcher ID: NA
- Scopus Author ID: NA
- Homepage: <https://ostad.nit.ac.ir/home.php?sp=370509>

### How to cite this paper:

R. Rouhani, S. E. Abdollahi, S. A. Gholamian, "Design of a synchronous reluctance motor with new hybrid lamination rotor structure," *J. Electr. Comput. Eng. Innovations*, 11(2): 243-252, 2023.

DOI: [10.22061/jecei.2022.8604.532](https://doi.org/10.22061/jecei.2022.8604.532)

URL: [https://jecei.sru.ac.ir/article\\_1803.html](https://jecei.sru.ac.ir/article_1803.html)

